SAND2006-3449P

Technical Reference on Hydrogen Compatibility of Materials

High-Alloy Ferritic Steels:
Duplex Stainless Steels (code 1501)

Prepared by:

J.A. Zelinski, Defense Nuclear Facilities Safety Board, Washington DC
and
C. San Marchi, Sandia National Laboratories, Livermore CA

Editors
C. San Marchi
B.P. Somerday
Sandia National Laboratories

This report may be updated and revised periodically in response to the needs of the technical community; up-to-date versions can be requested from the editors at the address given below or downloaded at http://www.ca.sandia.gov/matlsTechRef/ . The success of this reference depends upon feedback from the technical community; please forward your comments, suggestions, criticisms and relevant public-domain data to:

Sandia National Laboratories
Matls Tech Ref
C. San Marchi (MS-9402)
7011 East Ave
Livermore CA 94550.

This document was prepared with financial support from the Safety, Codes and Standards program element of the Hydrogen, Fuel Cells and Infrastructure program, Office of Energy Efficiency and Renewable Energy; Pat Davis is the manager of this program element. Sandia is a multiprogram laboratory operated by Sandia Corporation, a Lockheed Martin Company, for the United States Department of Energy under contract DE-AC04-94AL85000.

1. General

A duplex stainless steel is an alloy containing a two-phase microstructure of face-centered cubic austenite (α) and body-centered cubic ferrite (γ), where the phases each possess at least 12% Cr (by weight). Generally, duplex stainless steels have compositions in the range 18-26% Cr, 4-7% Ni, and in many cases 2-3% Mo with some nitrogen. The so-called super duplex stainless steels have alloy contents at (or even slightly greater than) the high end of these ranges. Duplex stainless steels are typically used in applications that benefit from their high resistance to stress corrosion cracking and chloride ion attack, good weldability, and greater strength than other stainless steels.

The solidification structure of duplex stainless steels makes them initially isotropic; however, typical processing routes for metals (drawing, rolling etc.) add significant anisotropy to their two-phase microstructure. Given this two-phase microstructure, duplex stainless steels provide a mixture of the properties of each phase so that they are tougher than the ferritic steels and stronger than the (annealed) austenitic steels by a factor of about two. This implies that their compatibility with hydrogen is also combined. Ferrite is highly susceptible to hydrogen-assisted fracture and has high diffusivity and low solubility for hydrogen. Austenite is generally much less susceptible to hydrogen-assisted fracture, but has a very high solubility and very low diffusivity for hydrogen. As a result, the austenite phase can act as a hydrogen reservoir with respect to the ferrite phase and the resistance to hydrogen-assisted fracture increases with austenite content [2]. A further consequence of the difference in transport of hydrogen in these two primary phases is that a fully ferritic steel recovers much of its ductility in a few days when removed from a hydrogen environment, while the presence of 15% austenite results in much less recovery after removal from a hydrogen environment [2]. No detectable recovery of ductility is noted in thermally precharged 2205 (35% austenite) after storage at ambient temperature for 3 years [2].

In general, duplex stainless steels with internal hydrogen experience significant losses in ductility as measured by reduction of area in smooth tensile tests [2-5]. Ductility losses when tested in low-pressure hydrogen gas are less, although quite significant considering the low hydrogen fugacity at low pressure. Effects in gaseous hydrogen are also manifest in notched specimens [6, 7] and fatigue [8, 9].

1.1 Composition

Table 1.1.1 lists the approximate composition ranges for a number of duplex alloys. Table 1.1.2 provides the composition of several heats of duplex stainless steel used to study hydrogen effects. Table 1.1.3 summarizes the nominal mechanical properties and austenite content of materials from several studies on hydrogen effects.

1.2 Common Designations

Duplex stainless steels are often designated with four digits, the first two digits representing the weight percent of chromium, and the second two digits representing the weight percent of nickel; thus 2205 nominally has 22% Cr and 5% Ni. Unlike other stainless steels, however, a number of duplex stainless steels have registered trademarks and tradenames associated with them such as Uranus 50, Zeron 100, and Ferralium 255. The more common alloys and their tradenames are summarized in Table 1.1.1.

2. Permeability, Diffusivity and Solubility

Hydrogen gas permeation experiments on duplex alloys have not been reported in the literature to our knowledge. Perng and Altstetter, however, have performed gas phase permeation experiments on highly cold-worked type 301 and type 304 stainless steels that resulted in microstructures with large fractions of α' martensite [10]; martensite and ferrite are expected to have relatively similar hydrogen transport properties since both phases are body-centered cubic (while austenite is face-centered cubic). Their results show the diffusivity of the 301 austenite-martensite composite increases with content of martensite and approaches the value measured for a ferritic stainless steel at high concentrations. The permeability of the 301 composites is also generally between the fully austenitic alloys (low permeability) and the ferritic stainless steel (high permeability), except at the highest martensitic contents where the permeability in the composite is greater than the ferritic stainless steel. The hydrogen solubility is the quotient of the permeability and the diffusivity, thus the hydrogen solubility of the composite material is again between the low solubility exhibited in the ferritic stainless steel and the high solubility in the austenitic alloys.

Electrochemical and off-gassing techniques have been used to determine the diffusivity of hydrogen atoms in duplex stainless steels. Because of the two-phase structure and, generally, anisotropic distribution of phases, hydrogen transport in duplex steels can be a function of orientation. Hutchings et al. [11, 12] found that hydrogen diffusivity in duplex stainless steel (heat H91) was greater when the hydrogen flux was parallel to the elongated grain structure, however, this effect was relatively modest: about a factor of two. They also report that the diffusivity is not strongly affected by austenite content (γ) in the range 44% to 15%, but the diffusivity increases rapidly as the material becomes fully ferritic. The ratio of diffusivity of the duplex alloy with no austenite and with 44% austenite, however, is about 400 [12]. This trend is consistent with the inverse rule of mixtures reported for diffusivity by Iacoviello et al. [13] of the form

$$\frac{1}{D_{eff}} = \frac{\left(1 - f_\gamma\right)}{D_\alpha} + \frac{f_\gamma}{D_\gamma} \qquad (1)$$

This is a variant of the form proposed elsewhere [14], where f_γ is the fraction of austenite and D_{eff} is the effective diffusivity of the alloy and D_i is the diffusivity of the individual phases. Similar to orientation effects and the effects of austenite content, cold-work was found to have only a small effect on diffusivity of 2205 duplex stainless steel [15]. The diffusivity reported in these and several other studies are given in Figure 2.1.

Degradation of tensile ductility due to precharging with hydrogen can be recovered if the materials are removed from the hydrogen environment and heated [3]. However, it may take an extraordinarily long time to recover properties without heating [2, 13]. Significant degradation in tensile ductility was found to remain in thermally precharged 2205 (~35% austenite) after 55 days [3] and 3 years [2] at room temperature, but nearly full recovery of ductility was achieved by heating at 573 K for 4 hours [3]. As described above, the hydrogen diffusivity is relatively

insensitive to phase distribution for expected ranges (γ content from 25 to 50% or greater), thus recovery of properties is not expected to be a strong function of the relative amounts of austenite and ferrite or their morphology.

The concentration of hydrogen in a 2205 duplex stainless steel with about 35% austenite content (heat Z91A) was found to be about 20 wppm after precharging in 22 MPa H_2 gas at 623 K for 48h [2, 5]. Thermal precharging at the same temperature but a slightly lower pressure (17 MPa) resulted in hydrogen content of 15 wppm [4]. These conditions are reported to be sufficient to reach uniform saturation in tensile bars with a gauge diameter of 3.2 mm [2, 4, 5].

3. Mechanical Properties: Effects of Gaseous Hydrogen

3.1 Tensile Properties

3.1.1 Smooth Tensile Properties

Room temperature testing of smooth tensile specimens with internal hydrogen (by thermal precharging in hydrogen gas) shows significant loss in ductility [2-5]. The relative reduction of area is commonly used to evaluate hydrogen-assisted fracture in smooth tensile specimens as shown in Figure 3.1.1.1 as a function of strain rate. This plot shows the general trend that susceptibility to hydrogen-assisted fracture is enhanced at low strain rates due to more time for hydrogen redistribution to susceptible features in the microstructure.

Smooth tensile specimens strained in hydrogen gas (external hydrogen) generally show (Figure 3.1.1.2) an increased susceptibility to hydrogen-assisted fracture as the hydrogen fugacity (i.e. pressure) is increased [3, 5]. For hydrogen pressure on the order of an atmosphere and less, the trend with respect to rate of deformation is not a continuous decrease in resistance to hydrogen-assisted fracture as strain rate is lowered (Figure 3.1.1.2). The observed minimum in ductility at intermediate strain rate has been interpreted as due to the effect of deformation rate on both hydrogen transport and martensitic transformations [5]. The role of martensitic transformations on hydrogen-assisted fracture in austenitic steels has not been fully resolved, but it appears that martensitic transformations, while perhaps not necessary for degradation of stainless steels in hydrogen environments [16], certainly exacerbate hydrogen-assisted fracture when they form [17]. Figure 3.1.1.3 compares the absolute RA for a single heat of 2205, showing that the ductility loss is a function of hydrogen fugacity.

Although it is expected that orientation of the microstructure in duplex stainless steels could play an important role in hydrogen-assisted fracture, tensile testing of 2205 pipe with internal hydrogen shows little affect of orientation [4]. Tensile specimens tested in low-pressure external hydrogen, however, do show some effect of orientation [3-5]. Moreover, banded microstructures show larger variations with orientation than comparatively equiaxed microstructures [4]. As described above, hydrogen transport appears to play a more significant role in ductility degradation for testing in low-pressure hydrogen compared to testing at higher pressures or with internal hydrogen. Since the diffusivity of hydrogen is much greater in ferrite, hydrogen transport along oriented ferrite will be significantly greater than hydrogen transport perpendicular to ferrite orientation. Moreover, orientation effects will probably become more

important as the ferrite content is decreased since there will be less contiguity of the ferrite perpendicular to the aligned microstructure.

3.1.2 Notched Tensile Properties

Notched tensile foils of Ferralium 255 (heat P88) suffer a significant reduction in notch tensile strength and elongation when tested in 0.11 MPa hydrogen gas compared to testing in air at ambient temperature [6]. At temperature ≥ 373 K, little change in properties is observed for these same conditions [6].

3.2 Fracture mechanics

3.2.1 Fracture toughness

No known published data in hydrogen gas.

3.2.2 Threshold stress-intensity factor

Altstetter et al. determined crack growth rates and threshold stress intensity values in notched sheet specimens of Ferralium 255 (heat P88) where plane stress conditions prevailed [6, 18]. Specimens were tested in up to 0.22 MPa hydrogen gas [6] and precharged to saturation in molten salts at temperature of 538 K (i.e., internal hydrogen) [18]. These studies found that threshold values decreased as hydrogen fugacity increased. The threshold values also increased as temperature increased for tests performed in hydrogen gas, particularly for tests at 348 K and 373 K [6].

Classic microvoid coalescence was observed on the fracture surfaces of precharged specimens at low hydrogen contents, while the amount of flat cleavage facets increased as the hydrogen content was increased. Testing temperature between 273 and 323 K had little effect on fracture properties with internal hydrogen.

3.3 Fatigue

Fatigue testing of a 2507 super duplex stainless steel (M92) in flowing hydrogen gas (i.e. hydrogen at approximately ambient pressure) resulted in crack growth rates that are almost order of magnitude higher than in argon for $\Delta K > 25$ MPa$\sqrt{m}$ with R = 0.5 (ratio of minimum to maximum K and load) [9]. The crack growth rates, however, were similar for small stress intensity range (ΔK), less than about 15 MPa$\sqrt{m}$ [9]. The upper and lower bounds of crack growth rates as a function of ΔK from Ref. [9] are shown in Figure 3.3.1. Crack growth rates also tended to be faster for greater R ratios although they become similar at $\Delta K > 30$ MPa$\sqrt{m}$ [9]. Fractography in this study showed that the ferrite failed by cleavage, and ferrite cleavage ahead of the crack tip was not observed. A subsequent study [8] found that temperature in the range 298 K to 453 K had little effect on fatigue crack growth rates in flowing hydrogen.

3.4 Creep

No known published data in hydrogen gas.

3.5 Impact

No known published data in hydrogen gas.

3.6 Disk rupture testing

Disk rupture tests have been performed on duplex alloys referred to as 326 [19] and IN744 [20]; these alloys appear to be similar with nominally 26Cr-7Ni and no molybdenum. Duplex stainless steel is classified as displaying little or no sensitivity to hydrogen in these studies and particularly attractive due to its high-strength [19]. This is at odds with other data from the literature, perhaps due to the relative short-time scales associated with the disk rupture tests precluding substantial hydrogen transport in the lattice.

4. Metallurgical considerations

4.1 Primary processing

Grain size effects have been studied for 2205 duplex stainless steel by slow strain rate testing in NaCl solution under cathodic potential. Coarser grained material (12-14μm) displayed a greater loss in ductility than fine-grained material (7-8μm) [21].

4.2 Heat Treatment

The resistance to hydrogen-assisted fracture of a 2205 duplex stainless steel (heat E96) was found to increase with austenite content in tensile testing in external hydrogen (0.2 MPa hydrogen gas) and with internal hydrogen (thermal precharging in 25 MPa hydrogen gas at 633 K). The duplex steel was thermally processed to produce between about 5 and 50% austenite and the RA (both with internal and external hydrogen) was found to drop from greater than 50% to less 20% as the amount of austenite was reduced (Figure 4.1.1) [2]. The trend for strain rate effects was similar for all microstructures (see Section 3.1.1). The effect of austenite content, however, must be balanced with the fact that the yield strength of the microstructures with high austenite contents were somewhat lower (600 MPa compared to 750 MPa) than the microstructure with low austenite content (Table 1.1.3); hydrogen effects tend to be more pronounced in higher strength alloys. Nevertheless, the observation that austenitic phases are more resistant to hydrogen-assisted fracture than other phases is consistent with the view that austenitic stainless steels are relatively resistant to hydrogen compared to other steels [22].

4.3 Properties of welds

Laser welded notched tensile specimens from 2205 plate (heat Y05) were tested in 0.2 MPa gaseous hydrogen and reported in Ref. [7]. The austenite content in the weld was varied by controlling the welding process and it was found that material with higher austenite content showed greater resistance to hydrogen. The notched tensile strength (σ_s) of the base material (43% austenitic) was reduced by 9% when testing in hydrogen gas, while the σ_s of a weld with only 25% austenite was reduced by 28% in hydrogen gas.

Hydrogen susceptibility of duplex stainless steel increases markedly when the delta ferrite content increases above 50% in weld deposits produced using an Ar-10 vol-% H_2 shielding gas [23]. Hydrogen-bearing shielding gases are used to improve weld pool fluidity and prevent surface oxidation, but hydrogen is entrapped in the microstructure during the welding process, increasing hydrogen susceptibility.

5. References

1. M Nystrom, B Karlsson and J Wasen. The mechanical properties of a duplex stainless steel. (1990).
2. AA El-Yazgi and D Hardie. Effect of heat treatment on susceptibility of duplex stainless steel to embrittlement by hydrogen. Mater Sci Technol 16 (2000) 506-510.
3. W Zheng and D Hardie. The effect of hydrogen on the fracture of a commercial duplex stainless steel. Corros Sci 32 (1991) 23-36.
4. W Zheng and D Hardie. Effect of structural orientation on the susceptibility of commercial duplex stainless steel to hydrogen embrittelement. Corrosion 47 (1991) 792-799.
5. AA El-Yazgi and D Hardie. The embrittlement of a duplex stainless steel by hydrogen in a variety of environments. Corros Sci 38 (1996) 735-744.
6. T-P Perng and CJ Altstetter. Cracking Kinetics of Two-Phase Stainless Steel Alloys in Hydrogen Gas. Metall Trans 19A (1988) 145-152.
7. MC Young, SLI Chan, LW Tsay and CS Shin. Hydroge-enhanced cracking of 2205 duplex stainless steel welds. Mater Chem Phys 91 (2005) 21-27.
8. TJ Marrow, PJ Cotterill and JE King. Temperature effects on the mechanism of time independent hydrogen assisted fatigue crack in duplex steels. Acta metall mater 40 (1992) 2059-2068.
9. TJ Marrow, CA Hippsley and JE King. Effect of mean stress on hydrogen assisted fatigue crack propagation in duplex stainless steel. Acta metall mater 39 (1991) 1367-1376.
10. T-P Perng and CJ Altstetter. Effects of Deformation on Hydrogen Permeation in Austenitic Stainless Steels. Acta metall 34 (1986) 1771-1781.
11. RB Hutchings, A Turnbull and AT May. Measurement of hydrogen transport in a duplex stainless steel. Scr Metall Mater 25 (1991) 2657-2662.
12. A Turnbull and RB Hutchings. Analysis of hydrogen atom transport in a two-phase alloy. Mater Sci Eng A177 (1994) 161-171.
13. F Iacoviello, M Habashi and M Cavallini. Hydrogen embrittlement in the duplex stainless steel Z2CND2205 hydrogen-charged at 200˚C. Mater Sci Eng A224 (1997) 116-124.
14. U Bernabai and R Torella. Thermal analysis of hydrogen-charged austenitic and duplex stainless steel. Int J Hydrogen Energy 18 (1993) 763-771.
15. SS Chen, TI Wu and JK Wu. Effects of deformation on hydrogen degradation in a duplex stainless steel. J Mater Sci 39 (2004) 67-71.
16. AW Thompson. Ductility Losses in Austenitic Stainless Steels Caused by Hydrogen. in: IM Bernstein and AW Thompson, editors. Proceedings of the International Conference on the Effects of Hydrogen on Materials Properties and Selection and Structural Design: Hydrogen in Metals, 1973, Champion PA. American Society of Metals (1974) p. 91-105.
17. G Han, J He, S Fukuyama and K Yokogawa. Effect of strain-induced martensite on hydrogen environment embrittlement of sensitized austenitic stainless steels at low temperatures. Acta mater 46 (1998) 4559-4570.
18. J-H Huang and CJ Altstetter. Cracking of Duplex Stainless Steel Due to Dissolved Hydrogen. Metallurgical and Materials Transactions 26A (1995) 1079-1085.
19. PF Azou and JP Fidelle. Very low strain rate hydrogen gas embrittlement (HGE) and fractography of high-strength, mainly austenitic stainless steels. in: MR Louthan, RP McNitt and RD Sisson, editors. Environmental Degradation of Engineering Materials III,

1987, The Pennsylvania State University, University Park PA. The Pennsylvania State University, University Park PA p. 189-198.

20. J-P Fidelle, R Bernardi, R Broudeur, C Roux and M Rapin. Disk Pressure Testing of Hydrogen Environment Embrittlement. in: Hydrogen Embrittlement Testing, ASTM STP 543, American Society for Testing and Materials. (1974) p. 221-253.
21. SL Chou and WT Tsai. Effect of grain size on the hydrogen-assisted cracking in duplex stainless steels. Mater Sci Eng A270 (1999) 219-224.
22. RJ Walter and WT Chandler. Influence of Gaseous Hydrogen on Metals: Final Report (NASA CR-124410). Rocketdyne for the National Aeronautics and Space Administration, Canoga Park CA (Oct 1973).
23. K Shinozaki, L Ke and TH North. Hydrogen cracking in duplex stainless steel weld metal. Welding Journal 71 (1992) S387-S396.
24. ASTM DS-56H, Metals and Alloys in the UNIFIED NUMBERING SYSTEM (SAE HS-1086 OCT01). American Society for Testing and Materials (Society of Automotive Engineers) (2001).
25. WC Luu, PK Liu and JK Wu. Hydrogen transport and degradation of a commercial duplex stainless steel. Corros Sci 44 (2002) 1783-1791.

Table 1.1.1. Composition of several common commercial duplex stainless steels [24].

UNS No	AISI No / Common Name	Fe	Cr	Ni	Mo	Cu	Mn	Si	C	N	other
S32101	LDX 2101	Bal	21.0 22.0	1.35 1.7	0.1 0.8	0.1 0.8	4.0 6.0	1.0 max	0.04 max	0.20 0.25	0.04 max P; 0.3 max S
S32205	2205	Bal	22.0 23.0	4.5 6.5	3.0 3.5	—	2.0 max	1.0 max	0.03 max	0.14 0.20	0.03 max P; 0.02 max S
S32304	2304	Bal	21.5 24.5	3.0 5.5	0.05 0.60	0.05 0.6	2.5 max	1.0 max	0.03 max	0.05 0.20	0.04 max P; 0.04 max S
S32404	Uranus 50 (Uranus B50)	Bal	20.5 22.5	5.5 8.5	2.0 3.0	1.0 2.0	2.0 max	1.0 max	0.04 max	0.2 max	0.03 max P; 0.01 max S
S32520	Uranus 52N+	Bal	24.0 26.0	5.5 8.0	3.0 4.0	0.5 2.0	1.5 max	0.8 max	0.03 max	0.20 0.35	0.035 max P; 0.02 max S
S32550	Ferralium 255	Bal	24.0 27.0	4.5 6.5	2.9 3.9	1.5 2.5	1.5 max	1.0 max	0.04 max	0.10 0.25	0.04 max P; 0.03 max S
S32750	SAF 2507	Bal	24.0 26.0	6.0 8.0	3.0 5.0	—	1.2 max	0.8 max	0.03 max	0.24 0.32	0.035 max P; 0.02 max S
S32760	Zeron 100	Bal	24.0 26.0	6.0 8.0	3.0 4.0	0.5 1.0	1.0 max	1.0 max	0.03 max	0.2 0.3	0.5-1.0 W; 0.03 max P; 0.01 max S
S32900	329	Bal	23.0 28.0	2.5 5.0	1.0 2.0	—	1.0 max	0.75 max	0.08 max	—	0.04 max P; 0.03 max S

Table 1.1.2. Composition of several heats of duplex stainless steels used to study hydrogen effects.

Heat	Alloy	Fe	Cr	Ni	Mo	Cu	Mn	Si	C	N	Other	Ref.
P88	Ferralium 255	Bal	26	5.5	3	1.6	nr	nr	nr	0.16	nr	[6]
H91	Uranus 50	Bal	21.6	6.3	2.51	0.77	0.63	0.87	0.06	nr	<0.01 P; 0.01 S	[11, 12]
M91	Zeron 100	Bal	24.04	6.827	3.77	0.626	0.77	0.175	0.024	0.215	0.025 P; 0.002 S; 0.625 W	[8, 9]
Z91A	2205	Bal	22.3	5.7	2.9	0.06	1.62	0.35	0.027	nr	0.021 P; <0.002 S	[4]
Z91B		Bal	22.9	5.2	3.12	0.03	0.99	0.5	0.016	nr	0.019 P; 0.002S	[3, 4]
E96	2205	Bal	23.0	5.0	3.0	nr	1.0	nr	nr	0.13	nr	[2, 5]
I97	Similar to 2205	Bal	22.78	5.64	2.5	0.15	1.43	0.39	0.03	0.13	0.028 P; 0.011 S	[13]
C99A	2205	Bal	22.15	5.28	3.11	—	1.58	0.53	0.024	0.19	0.028 P; 0.002 S	[21]
C99B		Bal	22.4	5.42	3.24	0.21	1.43	0.41	0.014	0.198	0.025 P; 0.004 S	
L02	2205	Bal	22.79	5.32	3	0.04	1.53	0.37	0.03	0.2	0.03 P; 0.03 S	[25]
Y05	2205	Bal	21.1	5.8	2.7	0.02	1.42	0.45	0.052	0.165	0.025 P; 0.022 S	[7]

nr = not reported

Table 1.1.3. Mechanical behavior of duplex stainless steels used to study hydrogen effects prior to hydrogen exposure.

Material	Austenite content (%)	Strain rate (s^{-1})	S_y (MPa)	S_u (MPa)	El_t (%)	RA (%)	Ref.
Z91A - L	37	10^{-4}	651	795	42	84	[4]
Z91A - T			634	785	41	74	
Z91B - L	35		620	740	36	85	
Z91B - T			600	710	39	83	
Z91B	35	—	577	766	36	87	[3]
E96	35	—	623	744	42	78	[5]
E96 - 50	50	3.7×10^{-6}	592	758	39.1	80.5	[2]
E96 - 15	15		704	807	30.6	64.7	
E96 - 0	0		743	844	19.9	51.7	

L = Longitudinal, T = Transverse

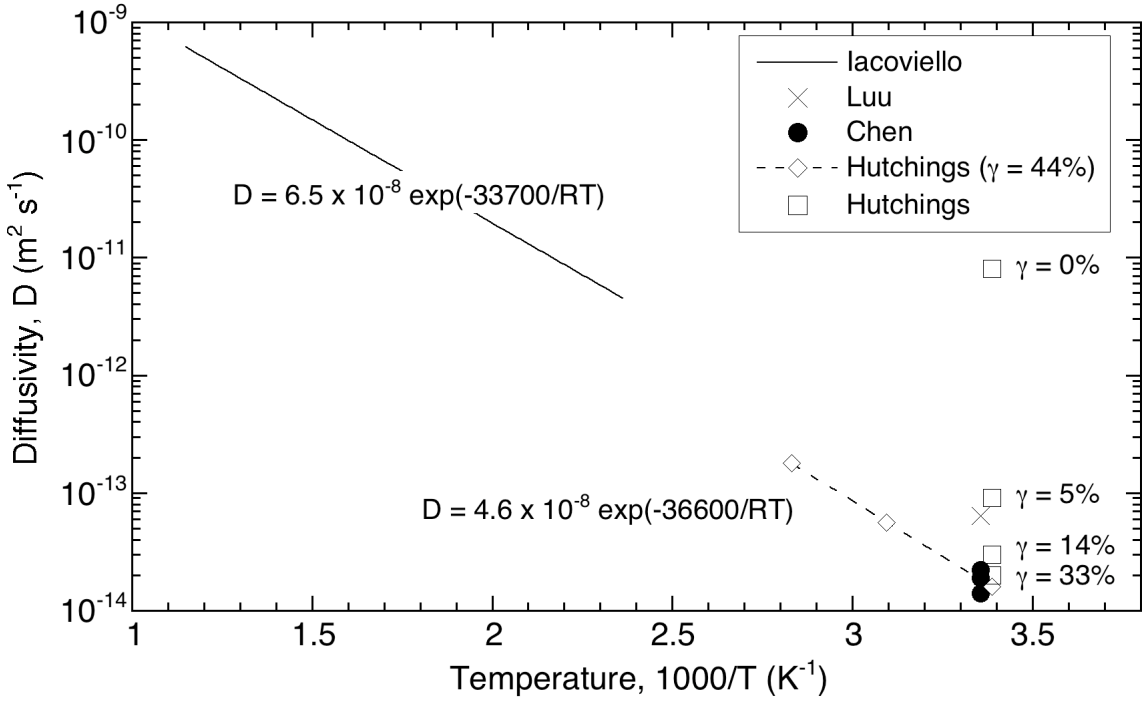

Figure 2.1. Hydrogen diffusivity as a function of temperature for several duplex alloys: Iacoviello, heat I97 [13]; Luu, heat L02 [25]; Chen, heat L02, values for annealed, cold-worked 20% and 40% respectively in increasing order of diffusivity [15]; Hutchings, heat H91 [11, 12].

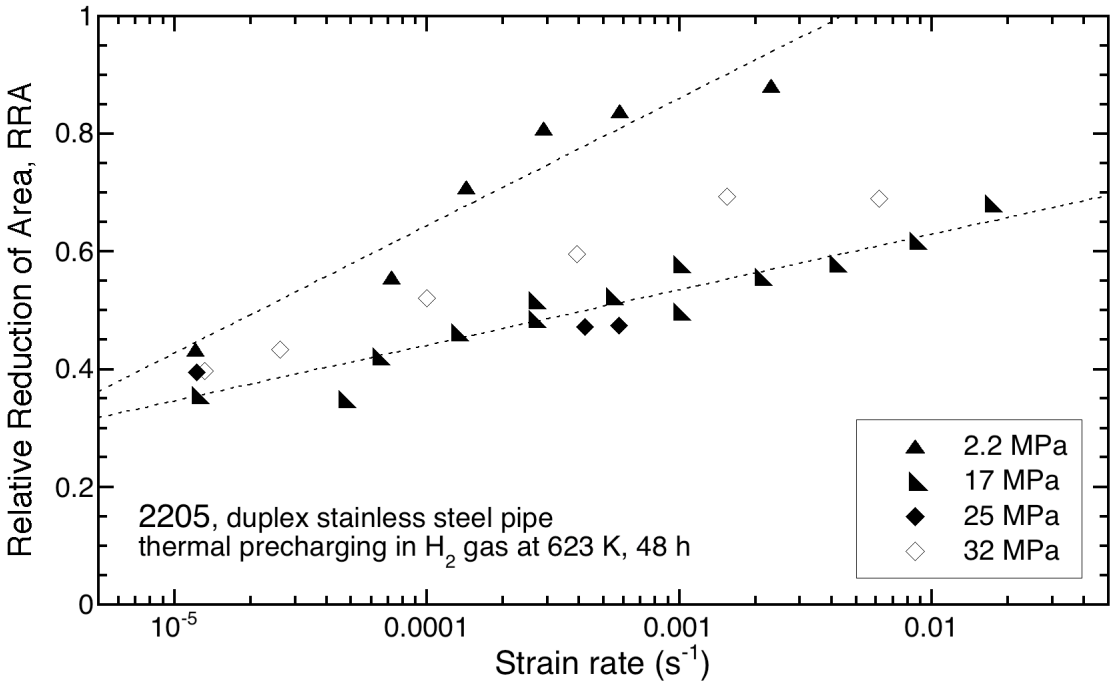

Figure 3.1.1.1. Relative reduction of area of 2205 duplex stainless as a function of stain rate in smooth tensile tests. The material has been thermally precharged with hydrogen at 623 K and several hydrogen gas pressures: closed symbols heat Z91B from Ref. [3]; open symbols heat E96 from Ref. [5].

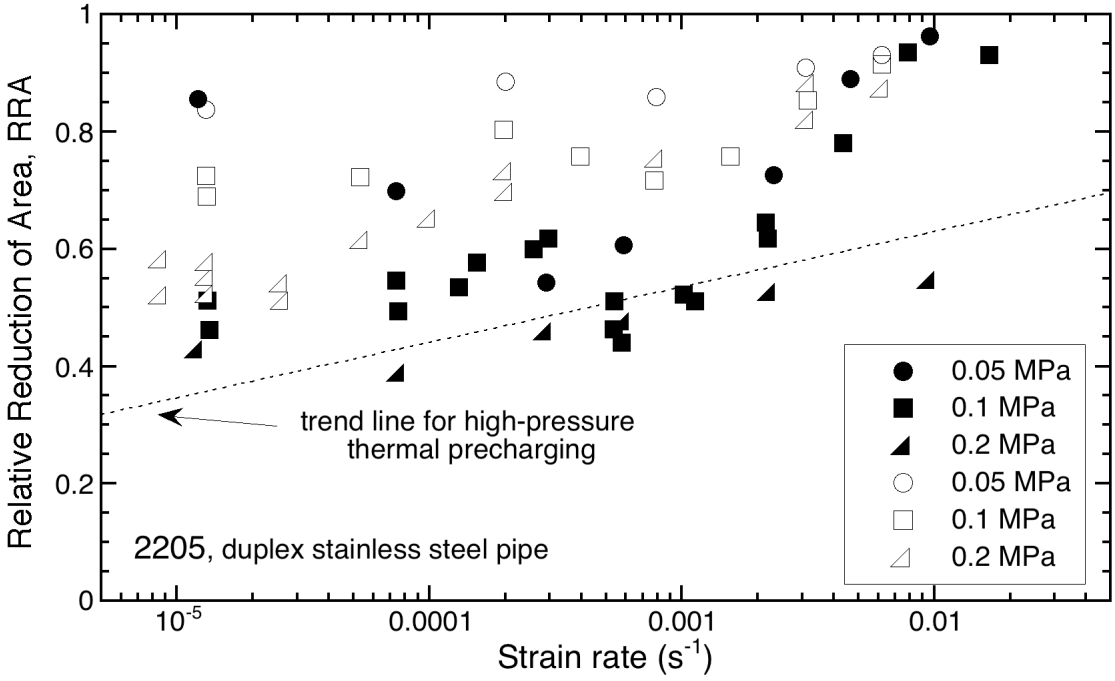

Figure 3.1.1.2. Relative reduction of area for 2205 duplex stainless as a function of stain rate in smooth tensile tests. Tests were conducted in hydrogen gas at room temperature and several hydrogen gas pressures: closed symbols heat Z91B from Ref. [3]; open symbols heat E96 from Ref. [5]. Trendline from Figure 3.1.1.1.

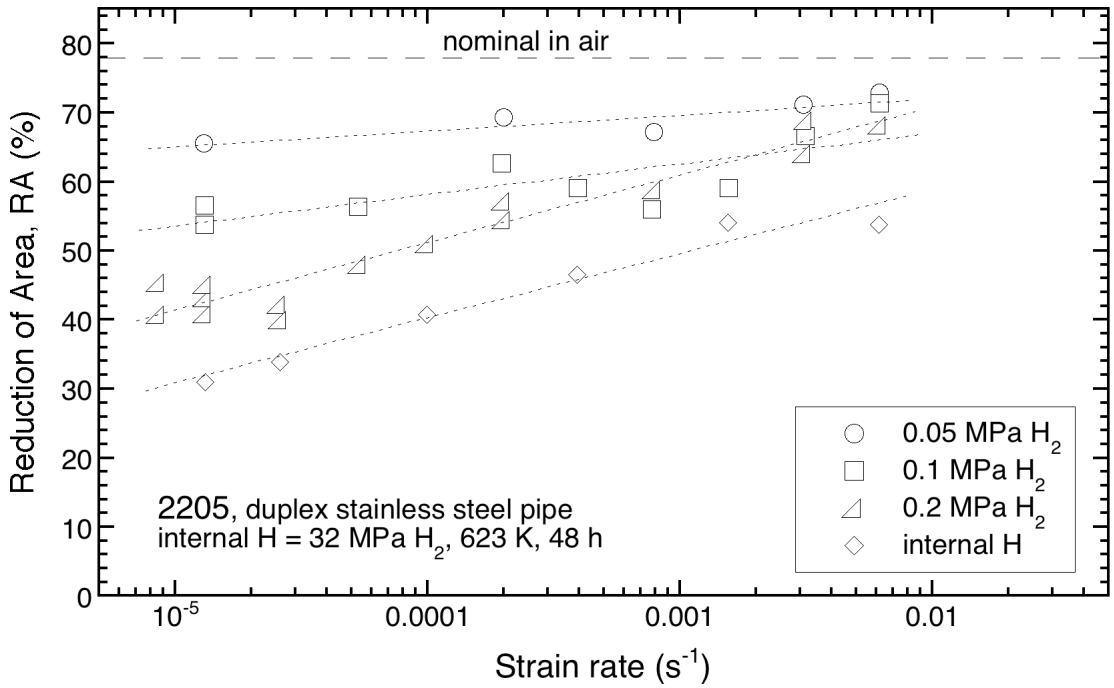

Figure 3.1.1.3. Reduction of area for 2205 duplex stainless (heat E96) as a function of stain rate in smooth tensile tests comparing internal and external hydrogen. Same data as from Figure 3.1.1.1 and 3.1.1.2. [5]

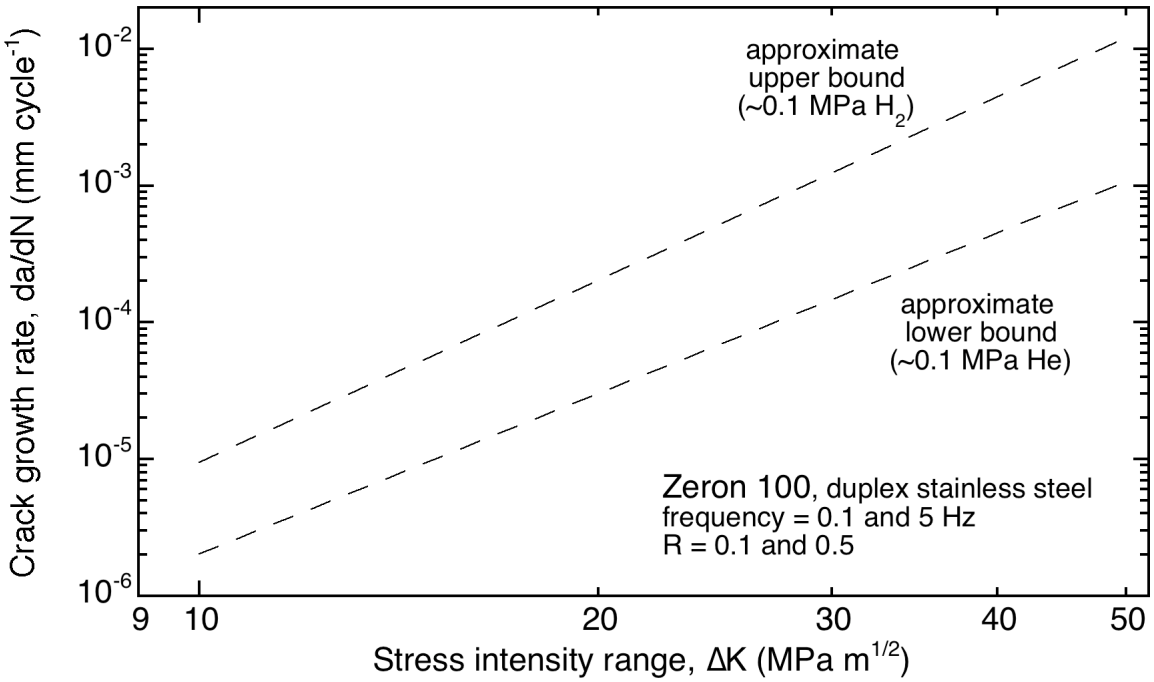

Figure 3.3.1. Approximate bounds for crack growth of compact tension specimens (heat M91) at 0.1 and 5 Hz in approximately ambient pressure, R = 0.1 and 0.5. [9]

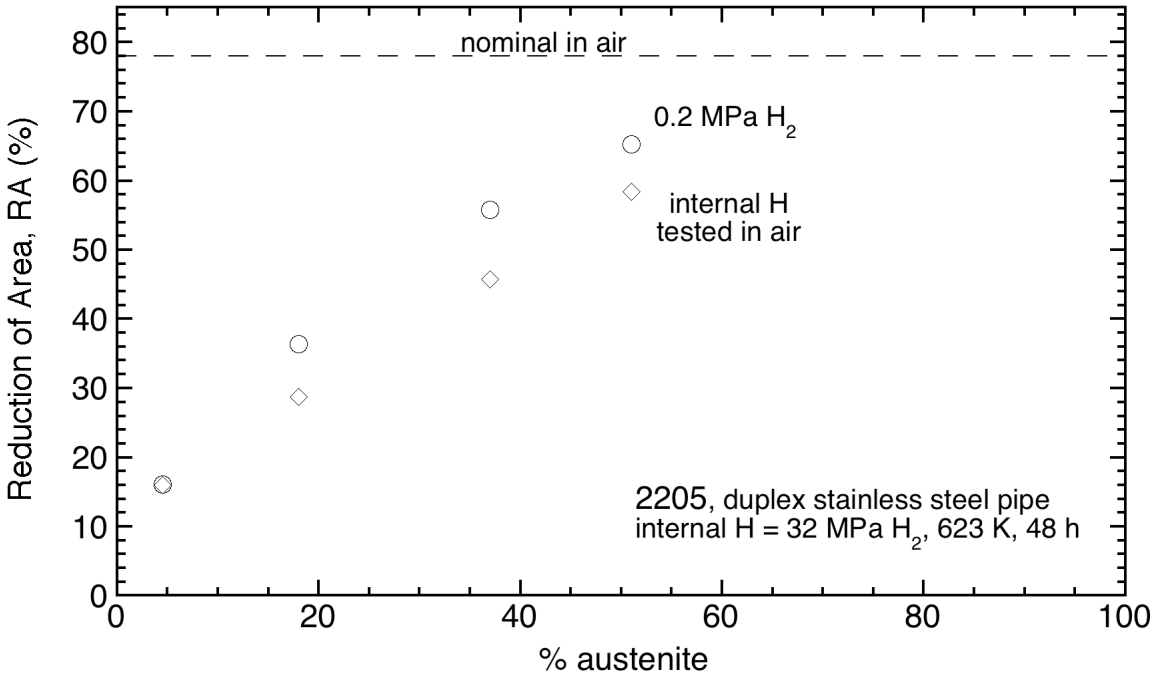

Figure 4.1.1. Reduction of area for 2205 duplex stainless steel (heat E96) as a function of austenite content with internal hydrogen and in external hydrogen. [2]